

POINCARÉ: A MULTI-BODY, MULTI-SYSTEM TRAJECTORY DESIGN TOOL

Mar Vaquero and Juan Senent

Mission Design and Navigation Section
NASA Jet Propulsion Laboratory, California Institute of Technology

ABSTRACT

Poincaré is a modular trajectory design tool based on a catalog of three-body science orbits and a differential corrector to compute connecting transfer arcs between orbits in multi-body systems. *Poincaré* attempts to offer a unified approach, i.e., an “all-in-one” integrated search within one interface and setup in MONTE (JPL’s signature astrodynamical computing platform.) The Science Orbit Design Tool facilitates rapid and well-informed decisions regarding the selection of periodic orbits for a particular mission and enables the simultaneous study of various orbit alternatives. The Reference Trajectory Design Tool allows the user to calculate optimal transfer paths from a departure orbit to a science orbit via dynamical systems structures (invariant manifolds and Poincaré maps), resulting in an end-to-end reference trajectory.

1. OVERVIEW

In the 1960’s, the application of insight from the circular restricted three-body problem (CR3BP) moved into the ‘space age’ when a mission to the Lagrange points was considered for NASA’s Apollo program. Since then, many of the structures that emerge in the CR3BP have been more actively exploited in trajectory design. Consequently, successful missions to the vicinity of the Lagrange points have since been launched, including the International Sun-Earth Explorer-3 (ISEE-3), the Solar Heliospheric Observatory (SOHO) [1], the Advanced Composition Explorer (ACE) [2], and the Microwave Anisotropy Probe (MAP) [3]. Parallel to the development of these mission concepts, the possibility of applying dynamical systems techniques to the design of these types of trajectories was also being considered. In fact, in the 1960’s, Conley had investigated low energy transfer orbits to the Moon using dynamical system techniques [4]. In the 1990’s, the use of invariant manifolds in the design process to construct pathways between the Earth and the Sun-Earth libration points was finally applied in an actual trajectory: the trajectory supporting the Genesis mission.

In recent years, the understanding of three-body dynamics within the astrodynamics community has improved tremendously, due in part to the increased utilization of techniques from dynamical systems theory [5, 6]. As a result, there exists a wide array of known orbits with significant potential for

parking, staging, and transfers within any three-body system (Fig. 1). However, the computation of such families of orbits and the corresponding connecting arcs is nontrivial and requires extensive knowledge of the dynamical mechanisms intrinsic to the system. The motivation for developing a tool like *Poincaré* at JPL was to provide a basic roadmap to allow any mission designer, with experience in multi-body dynamics or not, to construct an end-to-end trajectory with guidance and insight into the available dynamic structures.

There is significant interest in exploiting multi-body dynamics in the design of trajectories for robotic and human missions as demonstrated by MDEX and Discovery Program mission proposals – NEOCam [7] (Near-Earth Object Camera), FINESSE [8] (Fast Infrared Exoplanet Spectroscopy Survey Explorer), and Whipple [9], various NASA mission concepts – Europa Lander, Orion FT2, MoonRise [10], ARM [11] (Asteroid Redirect Mission), IMAP (Interstellar Mapping and Acceleration Probe), as well as in the design of extended and end-of-mission (spacecraft disposal) scenarios [12]. To aid in the design of such complex trajectories, *Poincaré* enables the selection, design, and implementation of a comprehensive catalog of science orbits along with connecting transfer arcs from a departure orbit in multi-body dynamical systems. *Poincaré* is currently focused on low energy trajectories and its development and implementation was split in three different, independent phases in the span of three years (2015-2018).

Phase I encompasses the design and implementation of a dynamic orbital catalog fully integrated in MONTE to guide the mission designer in the computation and selection of suitable science orbits that meet specific science requirements in a wide selection of three-body systems. The orbital catalog can be exploited in two different ways: i) via a direct approach, in which the analyst knows which orbit and parameters to select and, thus, possesses extensive knowledge of the dynamics of the CR3BP; and ii) via a guided approach, in which the user has a set of science requirements to be met but is unaware of all the available options. In this case, the user can browse the catalog and select the appropriate orbit based on a given set of parameters (stability, energy, amplitudes, etc). In both cases, after the preliminary design and selection process is complete, the tool provides a reference trajectory file containing states at specified epochs along with a full set

of orbital parameters describing the selected science orbit in either the three-body model or the full ephemeris model. A wide variety of multi-body orbits – over 800,000 orbits in the catalog, including 36 families of libration point orbits, moon-centered orbits and planar resonant orbits in seven 3-body systems – have been created and stored in an SQLite database.

During the second year of development (Phase II), dynamical systems techniques were implemented in the Reference Trajectory Design Tool to enable an end-to-end trajectory design. Invariant manifolds associated with unstable periodic orbits have been proven to be powerful transfer mechanisms between orbits. *Poincare* has the capability of 1) calculating stable and unstable manifold arcs allowing the user to interactively select a suitable transfer arc from a departure or parking orbit to the selected science orbit and 2) generating a Poincaré map from the stable and unstable manifold trajectories of a particular periodic orbit. In addition to providing a framework to calculate these dynamic structures, a powerful differential corrector module expands the use of the periodic orbit catalog. The differential corrections algorithm also allows the end-to-end trajectory design problem to be solved in a high fidelity model, i.e., the user-selected transfer arc and the science orbit are blended together resulting in a trajectory that is continuous in position and velocity; if a natural solution is not available (ΔV -free), correction maneuvers are added at specific locations along the trajectory. Additional constraints may be enforced on the trajectory, such as launch inclination, departure epoch, maximum time-of-flight, etc.

In Phase III, the *Poincare* modules developed in Phases I and II were merged to produce an end-to-end reference trajectory design tool. With the use of a robust differential corrections algorithm, selected transfer arcs and science orbits can be blended together resulting in the desired reference trajectory in any fidelity model. To aid the user in the design of ΔV -optimal transfer arcs between orbits, an invariant manifold module is available to compute and store any given number of stable and unstable manifold trajectories associated with a particular periodic orbit. In addition to the manifold module, the Poincaré map module helps the user in identifying suitable connections between trajectories both graphically and systematically.

Poincare modules and design features are detailed in the following sections. It is important to note that this paper is not intended to be a users manual, but rather a high-level overview of the tool's capabilities and restrictions. Complete information relevant to the tool's many functions along with tutorials and sample code can be found in the MONTE Documentation [13, 14, 15].

2. THE ORBITAL CATALOG

Poincare is currently focused on low energy trajectories and therefore, the Circular Restricted Three-Body Problem (CR3BP) serves as the basis for the problem formulation.

In the restricted problem, the motion of an infinitesimal third particle, P_3 , is modeled in the presence of two gravitationally-attracting bodies of significantly larger mass, P_1 and P_2 . The motion of P_3 is governed by the well-known scalar, second-order differential equations of motion in standard form [16],

$$\ddot{x} - 2\dot{y} - x = -\frac{(1-\mu)(x+\mu)}{d^3} - \frac{\mu}{r^3}(x-1+\mu) \quad (1)$$

$$\ddot{y} + 2\dot{x} - y = -\frac{(1-\mu)}{d^3}y - \frac{\mu}{r^3}y \quad (2)$$

$$\ddot{z} = -\frac{(1-\mu)}{d^3}z - \frac{\mu}{r^3}z \quad (3)$$

where d and r are evaluated as,

$$d = \sqrt{(x+\mu)^2 + y^2 + z^2}, \quad r = \sqrt{(x-1+\mu)^2 + y^2 + z^2} \quad (4)$$

The state vector \bar{x} is defined as the six-element state vector $[x \ y \ z \ \dot{x} \ \dot{y} \ \dot{z}]^T$, where the dot indicates a derivative with respect to the non-dimensional time, τ , and relative to an observer in a rotating reference frame. The mass fraction μ is associated with the two system primaries P_1 and P_2 , $\mu = \frac{m_2}{m_1+m_2}$, where m_1 and m_2 are the masses of P_1 and P_2 , respectively; P_2 is arbitrarily defined as the smaller primary such that $m_2 < m_1$. The form of these equations of motion (EOMs) does admit an integral labeled the Jacobi constant, C , that is, $V^2 = 2U^* - C$, where the speed relative to the rotating frame is denoted V . In this relative problem formulation, the parametric quantities are non-dimensionalized by the characteristic length, time, and mass. However, in MONTE, all state variables must be defined with the appropriate units of length, time, and mass. To bridge this gap, *Poincare* offers the capability of both dimensionalizing or non-dimensionalizing states as needed. Given these equations of motion and the differential equations governing the state transition matrix (STM), an initial state can be then numerically propagated to any future time using MONTE's DIVA propagator.

In 1892, French mathematician, theoretical physicist, engineer, and philosopher of science Jules Henri Poincaré – after whom this tool is named – proved that periodic orbits exist in the three-body problem. He also claimed that there are an infinite variety of periodic solutions [17]. For decades, and given the increasing speed and accuracy of modern computers, researchers have computed many families of periodic orbits in a variety of multi-body systems [18, 19, 20, 21, 22, 23, 24]. Lyapunov and halo orbits are common examples of planar and out-of-plane periodic motion near the libration points. Resonant orbits are periodic as well but, in contrast to Lyapunov or halo orbits, are not typically associated with a particular Lagrange point. Also a focus of interest lately are P_2 -centered orbits, such as distant retrograde orbits. Based on an extensive literature survey, the orbital catalog includes all known-to-date families of periodic orbits in a variety of

planet-satellite and Sun-planet systems. For robustness, the catalog is implemented in a self-contained, server-less, zero-configuration, transactional database engine, enabling a query of the catalog with tools other than MONTE. In fact, the catalog could be delivered as an independent, standalone product with no dependencies on MONTE.

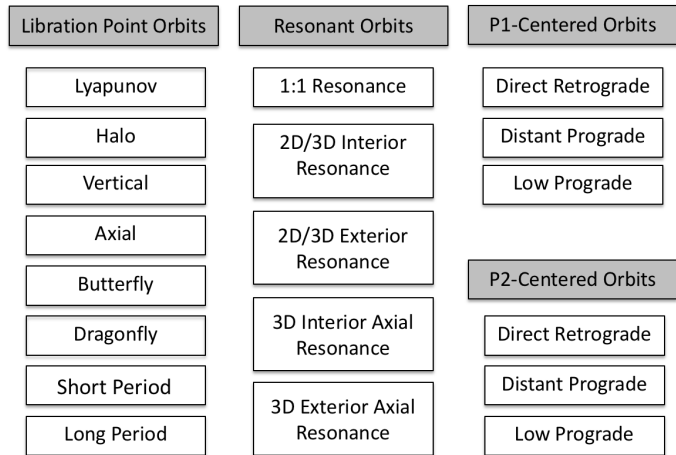


Fig. 1. General organization of well-known families of three-body orbits.

The computation of periodic motion in the CR3BP involves the use of a multi-dimensional version of a Newton-Raphson differential corrections process implemented as a shooting method. Planar, symmetric periodic orbits across the xz -plane can be calculated via a single shooting scheme that exploits symmetry properties. However, many periodic solutions exist in the CR3BP that do not possess a plane of symmetry. Additionally, convergence issues may arise if the integration times along the arcs are too long. As the variations are propagated, the linear approximation loses accuracy, so the sensitivities associated with the extended numerically integrated trajectory segments increase substantially. A multiple shooting algorithm is used to target these type of solutions.

In a multiple shooting algorithm, the trajectory is discretized into a series of “patch points” and multiple integrated segments are employed to satisfy the trajectory constraints. A patch point consists of the position and velocity on a trajectory at a specified time point. The segment of the trajectory between two temporally consecutive patch points is a trajectory leg. By using multiple legs, the sensitivities associated with a longer numerical propagation are reduced by integrating over smaller segments. Another advantage of multiple shooting schemes is the ability to apply path constraints at any patch points, generally allowing more control over the entire trajectory. The same multiple shooting formulation, implemented in MATLAB, was exploited to produce every periodic orbit available in the *Poincare* catalog. To create a family from an initial periodic orbit, a pseudo-arclength con-

tinuation scheme was employed, which is a special type of single-parameter continuation method [25]. This approach is based on the selection of a specific continuation parameter that may not be a physical quantity. Rather, the parameter is constructed to follow the evolution of the family of orbits that may not be a predetermined direction in configuration space. Implementing this continuation method involves stepping along the parameter values by fixing this parameter with an additional constraint. The families of periodic orbits currently stored in the *Poincare* SQLite database are listed below:

- L_1, L_2, L_3 Lyapunov orbits
- L_1, L_2, L_3 northern and southern Halo orbits
- L_1, L_2, L_3 Vertical orbits
- L_1, L_2, L_3 Axial orbits
- L_4, L_5 Long Period orbits
- L_4, L_5 Short Period orbits
- L_4, L_5 Vertical orbits
- L_4, L_5 Axial orbits
- Northern and southern Butterfly orbits
- Northern and southern Dragonfly orbits
- Distant Retrograde orbits
- Distant Prograde orbits
- Eastern and western Low Prograde orbits
- Resonant orbits (1:1, 1:2, 1:3, 1:4, 2:1, 2:3, 3:1, 3:2, 3:4, 4:1, 4:3)

For illustration purposes only, a selection of families of resonant, libration point, and moon-centered orbits is represented in Figs. 2-4. Each of these families of periodic orbits is available in the following 7 three-body systems:

- Sun-Earth system
- Sun-Mars system
- Earth-Moon system
- Mars-Phobos system
- Jupiter-Europa system
- Saturn-Titan system
- Saturn-Enceladus system

The parameters stored in the catalog are the same for every orbit:

- Gravitational parameter, μ
- Primary and secondary bodies
- Initial state (position and velocity)
- Orbital period
- Jacobi constant
- Eigenvalues of the monodromy matrix
- Stability index, ν

The stability index and eigenvalues of the monodromy matrix (state transition matrix evaluated after precisely one orbital revolution) are given as a measurement of the orbital stability and to aid the user in the search for an orbit with specific characteristics. As stated in Lyapunov’s Theorem [26], the eigenvalues of the monodromy matrix appear in reciprocal pairs.

In the CR3BP, the second-order system possesses three degrees of freedom and, thus, the monodromy matrix is defined in terms of six eigenvalues. For a periodic orbit to exist in the CR3BP, a minimum pair of eigenvalues must be equal to one because of the reciprocal nature of the eigenvalues. The monodromy matrix is a real matrix, so its eigenvalues are real or, if complex, appear in complex conjugate pairs on the unit circle. In general, a periodic orbit is defined as:

- unstable if $|\lambda| > 1$, i.e., the magnitude of the eigenvector goes to infinity as time goes to infinity,
- stable if $|\lambda| < 1$, i.e., the magnitude of the eigenvector approaches zero as time goes to infinity.

If the magnitude of the eigenvector does not change, i.e., $|\lambda| = 1$, the eigenvalue corresponds to the center subspace. The stability index is an alternative design parameter to better represent the stability characteristics associated with a given periodic orbit and leverage the fact that the eigenvalues occur in reciprocal pairs. The stability index, ν , is defined as,

$$\nu = \frac{1}{2} \left(|\lambda| + \left| \frac{1}{\lambda} \right| \right) \quad (5)$$

where λ is the eigenvalue of the monodromy matrix that possesses the largest modulus [27, 28]. If the stability index is less than or equal to one, that is, $|\nu| \leq 1$, then, the periodic orbit is considered to be marginally stable, in which case the corresponding eigenvalues do not yield stable and unstable invariant manifolds. For application purposes, the periodic orbits possessing this type of stability index do not allow for transfers shadowing invariant manifolds to and from the orbit. However, these orbits are great candidates for long-term or quarantine-type applications. Similarly, if $|\nu| \geq 1$, the periodic orbit includes an eigenvalue with magnitude greater than one, and its associated stable and unstable invariant manifolds can be computed [27, 20]. Moreover, the size of the stability index determines how fast the invariant manifolds approach or depart the orbit and, thus, this information is very useful in transfer design. Note that the database is designed to easily accommodate the addition of new families of periodic orbits as they become available.

The interface for this first module, including the dynamical model, orbital catalog and propagator, is simple. The content of the SQLite database can be viewed with the `poincare.printSummary()` command (screen output shown in Fig. 5), and queried by parameter, such as family name, energy range, stable vs. unstable, etc. by calling `poincare.queryDB()` and specifying the search criteria. Once the initial conditions are selected, the CR3BP MONTE Python class provides the appropriate dynamical environment with minimum intuitive setup by simply calling `poincare.makeCR3BP()` and specifying the primary and secondary bodies. If known, the gravitational parameter, μ , can be specified by the user; alternatively and by default,

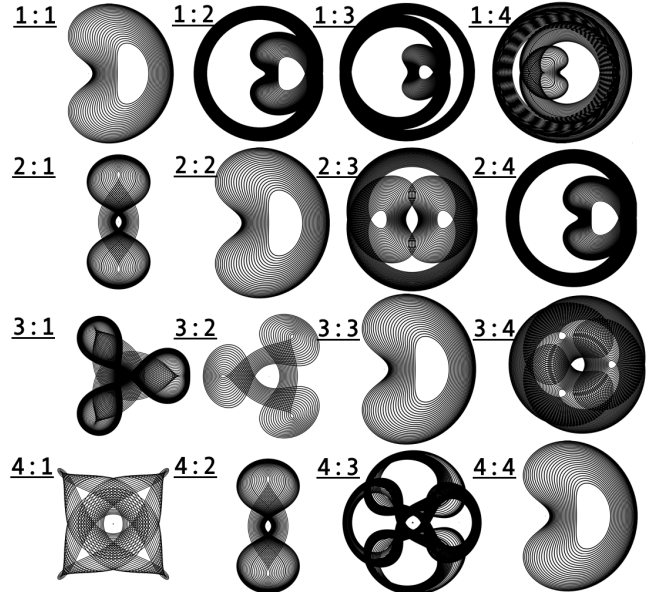


Fig. 2. Planar resonant orbits in the Earth-Moon system

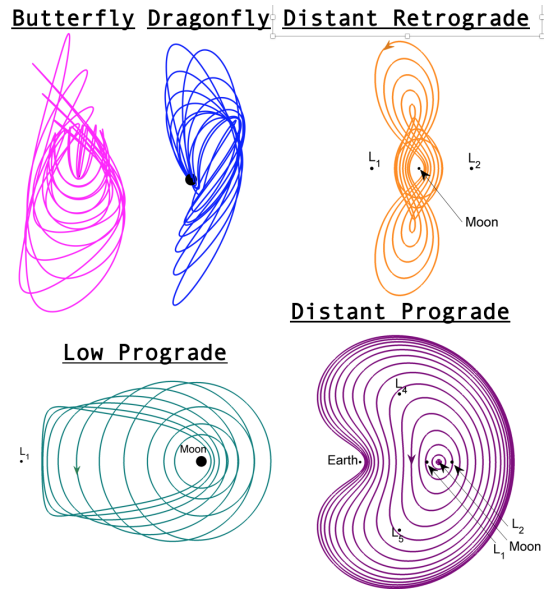


Fig. 3. P2 centered orbits plotted in the Earth-Moon system

Poincare calculates the value given ephemeris data and an assumed epoch. In addition, a third way to compute μ is also available by letting the user specify the initial epoch. If needed, the initial conditions can be dimensionalized by calling `poincare.makeDimensional()`. Once the dynamical model is created, *Poincare* also offers a simplified interface to the DIVA propagator in MONTE to quickly integrate a set of initial conditions from the catalog by calling `poincare.propagate()`. Subsequently, a complete set of outputs is saved in a standard BOA format.

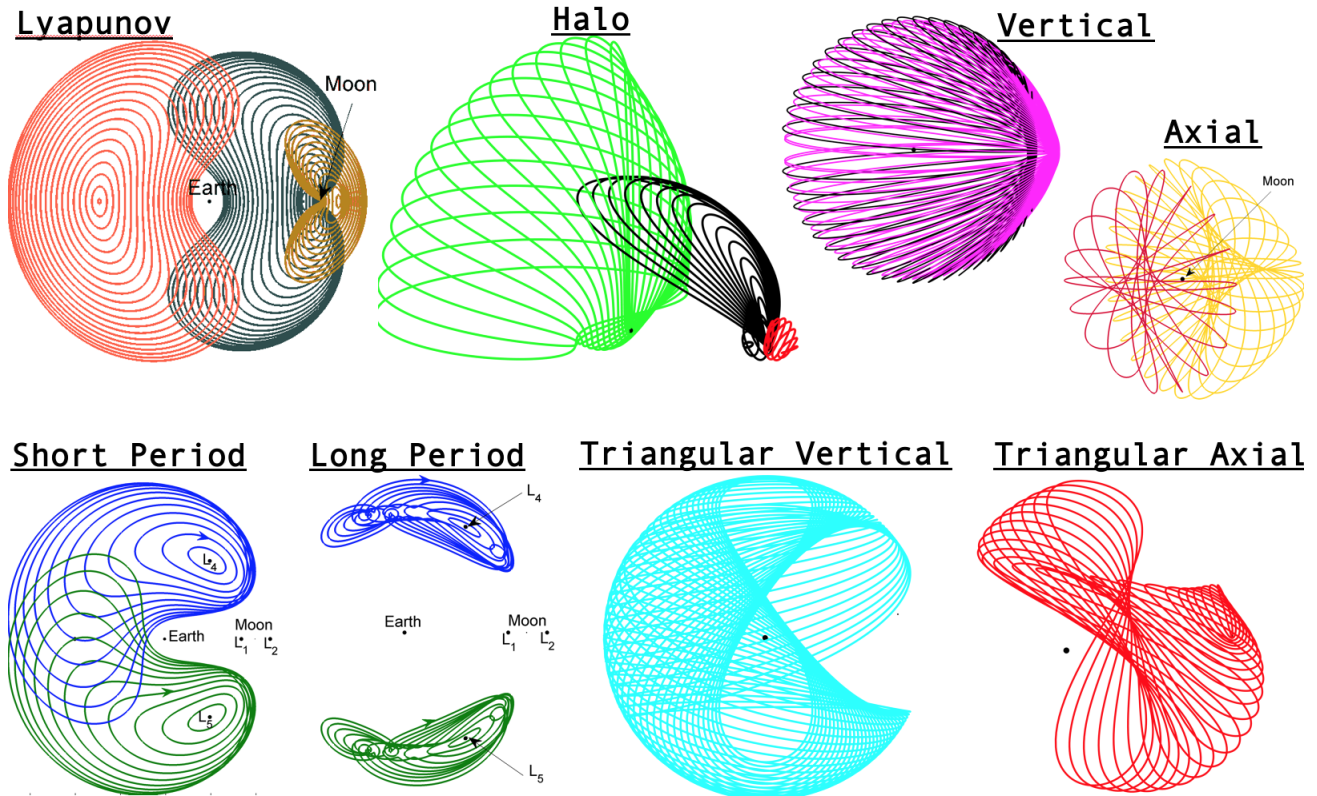


Fig. 4. Representative orbits in families of libration point orbits plotted in the Earth-Moon system rotating frame.

3. THE DIFFERENTIAL CORRECTOR

The *Poincare* CR3BP class offers a wide selection of pre-calculated and stored periodic orbits and the tools necessary to propagate and visualize the trajectories stored in the catalog. However, if the user is looking for a specific orbit that is not available in the catalog, or wishes to modify a given parameter, such as the Jacobi constant value, then a differential corrections scheme is needed. In a differential corrections process, a trajectory is defined as a series of time-based patch points and trajectory legs. The general scheme appears in Fig. 6 with the representation of an initial guess in Fig. 6(a) and a converged solution in Fig. 6(b). Note that the initial path, represented via a series of intermediate arcs, is discontinuous in position and velocity. The end goal is to employ the corrections algorithm to enforce continuity in all states, that is, position, velocity, and time.

The *Poincare* differential corrector module primarily utilizes COSMIC [29] and the MONTE Optimization Toolbox, enabling the user to set-up virtually any problem with any constraints. However, the interface has been designed to allow the user to quickly solve the following common problems with minimal coding effort:

- computing a specific periodic orbit within the families of orbits currently available in the catalog by selecting

a specific Jacobi constant value, period, or size element such as y-amplitude or z-amplitude,

- computing quasi-periodic orbits in the three-body model based on a particular periodic orbit by selecting the number of revolutions or amplitude (e.g. a Lissajous orbit),
- computing quasi-periodic orbits in a real ephemeris system starting from a periodic orbit in the CR3B model.

The interface for the differential corrector is fairly simple. The first step involves defining patch points, which is done with `poincare.corrector.makePatchPoints()`. The user specifies the number of patch points and the time interval between these. The corrector class is then created with `poincare.Corrector()` and the problem is solved by simply calling `poincare.corrector.solve()`. By default, the differential corrector is set up to enforce continuity conditions in position, velocity, and time between every patch point. The additional periodicity constraint, which forces the state of the initial and final patch points to be the same within the specified tolerance, can be added by calling `corrector.addClosedOrbitConstraints()`. Path constraints can be added to specific patch points. Say the user retrieves a distant retrograde orbit from the orbital catalog but wishes to modify the amplitude of the orbit such

PRIMARY_BODY	SECONDARY_BODY	TYPE	FAMILY	N OF ORBITS
SATURN	ENCELADUS	RESONANT	RES11	1335
SATURN	ENCELADUS	RESONANT	RES12	914
SATURN	ENCELADUS	RESONANT	RES13	1222
SATURN	ENCELADUS	RESONANT	RES21	595
SATURN	ENCELADUS	RESONANT	RES23	434
SATURN	ENCELADUS	RESONANT	RES31	320
SATURN	ENCELADUS	RESONANT	RES34	462
SATURN	ENCELADUS	LIBRATION_POINT	DPO	1678
SATURN	ENCELADUS	LIBRATION_POINT	DRO	1564
SATURN	ENCELADUS	LIBRATION_POINT	DRAGONFLY_NORTHERN	1911
SATURN	ENCELADUS	LIBRATION_POINT	DRAGONFLY_SOUTHERN	1911
SATURN	ENCELADUS	LIBRATION_POINT	L1_AXIAL	999
SATURN	ENCELADUS	LIBRATION_POINT	L1_HALO_NORTHERN	430
SATURN	ENCELADUS	LIBRATION_POINT	L1_HALO_SOUTHERN	430
SATURN	ENCELADUS	LIBRATION_POINT	L1_LYAPUNOV	2666
SATURN	ENCELADUS	LIBRATION_POINT	L1_VERTICAL	2516
SATURN	ENCELADUS	LIBRATION_POINT	L2_AXIAL	1005
SATURN	ENCELADUS	LIBRATION_POINT	L2_BUTTERFLY_NORTHERN	1518
SATURN	ENCELADUS	LIBRATION_POINT	L2_BUTTERFLY_SOUTHERN	1518
SATURN	ENCELADUS	LIBRATION_POINT	L2_HALO_NORTHERN	4488
SATURN	ENCELADUS	LIBRATION_POINT	L2_HALO_SOUTHERN	4488
SATURN	ENCELADUS	LIBRATION_POINT	L2_LYAPUNOV	2648
SATURN	ENCELADUS	LIBRATION_POINT	L2_VERTICAL	2099
SATURN	ENCELADUS	LIBRATION_POINT	L3_AXIAL	2184
SATURN	ENCELADUS	LIBRATION_POINT	L3_HALO_NORTHERN	702
SATURN	ENCELADUS	LIBRATION_POINT	L3_HALO_SOUTHERN	702
SATURN	ENCELADUS	LIBRATION_POINT	L3_LYAPUNOV	2699
SATURN	ENCELADUS	LIBRATION_POINT	L3_VERTICAL	3529
SATURN	ENCELADUS	LIBRATION_POINT	L4_AXIAL	475
SATURN	ENCELADUS	LIBRATION_POINT	L4_SHORT	4559
SATURN	ENCELADUS	LIBRATION_POINT	L4_VERTICAL	938
SATURN	ENCELADUS	LIBRATION_POINT	L5_AXIAL	475
SATURN	ENCELADUS	LIBRATION_POINT	L5_SHORT	4559
SATURN	ENCELADUS	LIBRATION_POINT	L5_VERTICAL	938
SATURN	ENCELADUS	LIBRATION_POINT	LPO_EASTERN	384
SATURN	ENCELADUS	LIBRATION_POINT	LPO_WESTERN	220
SATURN	ENCELADUS	LIBRATION_POINT	L4_LONG	242
SATURN	ENCELADUS	LIBRATION_POINT	L5_LONG	242

Fig. 5. Screen output of database content for the Saturn-Enceladus system only by calling `poincare.printSummary()`; the last column indicates the total number of orbits contained in each family.

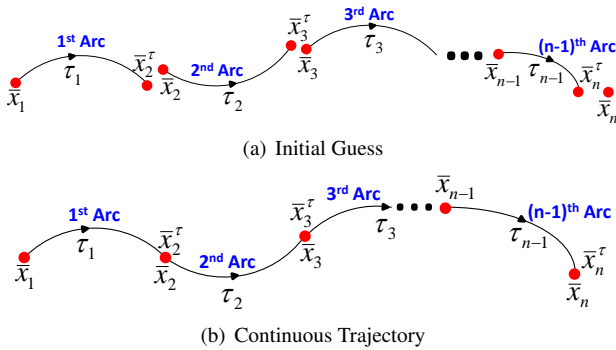


Fig. 6. Schematic of a general multiple shooting algorithm

that the maximum y-component is 1000 km larger. Then, `corrector.addConstraint[Cartesian.y()]` will do so. There are a variety of optimizers available to solve the problem, and the choice of one or another is application and problem dependent: DBLSE (Double Precision Bounded Least Squares with Equality Constraints), SNOPT (Sparse Non-Linear Optimizer), IPOPT (interior Point Optimizer), and SLSQP (Sequential Least Squares Programming). To aid the user in assessing the progress, standard screen output is printed with information relevant to the objective function,

bounds and control parameters. This output is also color-coded to help the user quickly identify problematic variables or constraints: blue indicates that the highlighted control parameter is close to the bound and red represents a constraint violation. Once the differential corrections process is completed, a set of outputs is given in a standard BOA format.

4. MANIFOLDS AND POINCARÉ MAPS

Invariant manifolds associated with periodic orbits in the vicinity of the libration points have been demonstrated to be efficient mechanisms for transport. That is, stable manifold trajectories are used in trajectory design as a means for a spacecraft to approach a particular periodic orbit by using just a small perturbation in the stable direction; similarly, unstable manifold trajectories can be exploited to depart a periodic (science) orbit by moving along the unstable direction, as illustrated in Fig. 8. The manifold module in *Poincare* provides a user-defined number of stable and unstable manifold trajectories associated with a particular periodic orbit in a BOA format. The user can select the propagation time for each manifold trajectory, the perturbation parameter, and number of manifold trajectories to be integrated. The selected number of invariant manifold trajectories propagated can vary drastically depending on the application. Storage of this potentially large number of trajectories in a single file can be a nontrivial task. To alleviate the problem of ending up with prohibitively large trajectory files, the *Poincare* manifold module is designed to save only the initial conditions associated with each propagated manifold trajectory as well as the dynamical system setup in a standard BOA format. Then, future re-integration and post-processing of these trajectories becomes a trivial task with the aid of the *Poincare* simple propagator.

An efficient method to calculate the manifold trajectories is by stepping off in the direction of the eigenvector corresponding to an eigenvalue of magnitude greater than one in the direction of the local unstable manifold, and in the eigenvector corresponding to an eigenvalue less than one in the direction of the local stable manifold. The key parameter in this process is the size of this step, or perturbation: if it is too large, the computed initial state is not a good approximation to the manifold and if it is too small, the trajectory spends too long near the periodic orbit and the integration error accumulates with little progress along the path. In general, manifolds for orbits that are more unstable depart or approach the orbit faster than the manifolds associated with orbits possessing a smaller stability index, so the size of the stability index can help in determining feasible transfer opportunities to and from the given orbit. However, ν is not sufficient to determine the size of the perturbation, which is also three-body system dependent. The *Poincare* manifold module allows the user to specify this parameter manually, but also offers a systematic

```

7 Cosmic/CORRECTOR/P1/X -1.151972689405265e+04 *km -1.151972689405265e+04 *km -1.519726894052646e+03 *km
15 Cosmic/CORRECTOR/P2/Y 9.604395582072197e+03 *km 1.955322770694432e+04 *km 1.960439558207220e+04 *km
-----
9 P0->P1 State: Y -1.000000000000000e+00 *km 1.026111093939107e+00 *km 1.000000000000000e+00 *km
11 P0->P1 State: DX -1.000000000000000e-05 *km/sec -1.111131090636430e-05 *km/sec 1.000000000000000e-05 *km/sec
15 P1->P2 State: Y -1.000000000000000e+00 *km 1.063062499204534e+00 *km 1.000000000000000e+00 *km
20 P2->P3 State: X -1.000000000000000e+00 *km -1.005207620703004e+00 *km 1.000000000000000e+00 *km
23 P2->P3 State: DX -1.000000000000000e-05 *km/sec -1.104945924335077e-05 *km/sec 1.000000000000000e-05 *km/sec
24 P2->P3 State: DY -1.000000000000000e-05 *km/sec -1.009549871732254e-05 *km/sec 1.000000000000000e-05 *km/sec
-----
Problem: CORRECTOR
Optimizer: DBLSE
Status: NOT_SET
Iterations: 5
=====
TOTAL( SUM ) 0.000000000000000e+00
-----
7 Cosmic/CORRECTOR/P1/X -1.151972689405265e+04 *km -1.151972689405265e+04 *km -1.519726894052646e+03 *km
15 Cosmic/CORRECTOR/P2/Y 9.604395582072197e+03 *km 1.955334137018752e+04 *km 1.960439558207220e+04 *km
-----
17 P1->P2 State: DX -1.000000000000000e-05 *km/sec -1.000001326710749e-05 *km/sec 1.000000000000000e-05 *km/sec
23 P2->P3 State: DX -1.000000000000000e-05 *km/sec -1.000002003226363e-05 *km/sec 1.000000000000000e-05 *km/sec
-----
Problem: CORRECTOR
Optimizer: DBLSE
Status: CONVERGED
Iterations: 6
=====
TOTAL( SUM ) 0.000000000000000e+00
-----
7 Cosmic/CORRECTOR/P1/X -1.151972689405265e+04 *km -1.151972689405265e+04 *km -1.519726894052646e+03 *km
15 Cosmic/CORRECTOR/P2/Y 9.604395582072197e+03 *km 1.955334136972732e+04 *km 1.960439558207220e+04 *km

```

Fig. 7. Representative output per iteration in the *Poincare* differential corrections process. In this run, P1 and P2 represent two patch points along a DRO orbit and X, Y, Z, DX, DY, DZ are position and velocity variables. The color blue indicates that the highlighted control parameter is close to the bound and red represents a constraint violation.

method to calculate the size of the perturbation tailored to the selected orbit. The implemented algorithm to do so is simple. Given the initial conditions and period of a periodic orbit (\mathbf{x}_0, T) along with a perturbation direction ($\hat{\mathbf{d}}$) associated with a stable or unstable eigenvector of the monodromy matrix (\mathbf{M}) and a perturbation step size (ϵ), an estimation of the error achieved after one orbit period can be calculated as follows,

$$\tilde{\mathbf{e}}(T) = \epsilon \mathbf{M} \hat{\mathbf{d}} = \epsilon \Phi(t_0, t_0 + T) \hat{\mathbf{d}}$$

The actual error can be calculated by propagating the initial conditions,

$$\mathbf{x}(T) = \text{propagate}_{t_0 \rightarrow t_0+T}(\mathbf{x}_0 + \epsilon \hat{\mathbf{d}}) \rightarrow \mathbf{e}(T) = \mathbf{x}(T) - \mathbf{x}_0$$

For realistic trajectory design purposes, it is desired to compute the maximum ϵ value that guarantees that the estimated position error is close to the actual position error. That is, the goal is to maximize ϵ such that,

$$\text{relError}(\mathbf{e}_r(T), \tilde{\mathbf{e}}_r(T)) < \text{relTol}$$

or

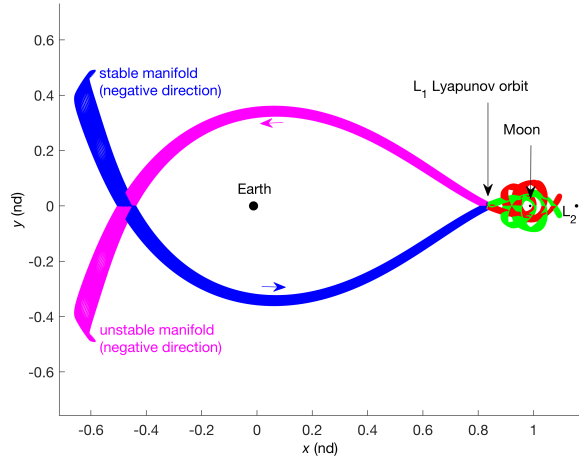
$$\text{absError}(\mathbf{e}_r(T), \tilde{\mathbf{e}}_r(T)) < \text{absTol}$$

This algorithm is robust for perturbation directions $\hat{\mathbf{d}}$ associated with unstable eigenvectors. For the case of stable eigenvectors, and in order to avoid numerical problems, it is necessary to use \mathbf{M}^{-1} and propagate backwards in time $-T$.

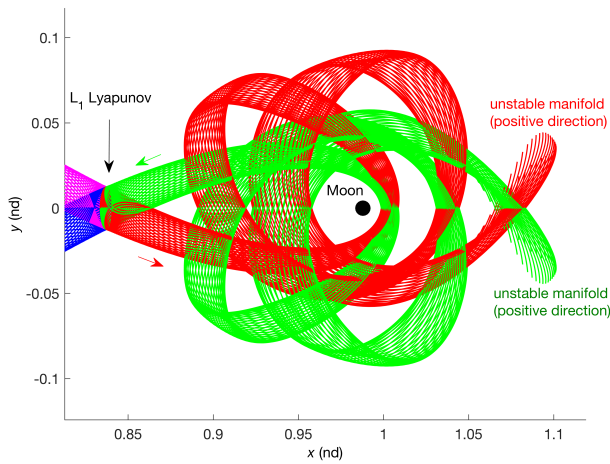
Again, the more experienced user can select a particular perturbation value, but with this algorithm, a suitable value is automatically calculated and it is tailored to each specific orbit and three-body system.

Poincaré maps can be used to display the stable and unstable manifold trajectories. The structures and intersections formed in the map can then be employed as a design tool to construct trajectories with predetermined characteristics (impact, short-term capture, long-term capture, etc.) In simple terms, a Poincaré map (named after Henri Poincaré) is the intersection of an orbit in the state space of a continuous dynamical system with a certain lower-dimensional subspace, called a Poincaré section or surface of section, which is transversal to the flow of the system [30]. *Poincare* offers the capability to generate maps from the stable and unstable manifold trajectories of a particular periodic orbit. The user defines the surface of section, or event, to construct the map and the propagation time. Then, a map can be formed by recording each time a trajectory reaches the specified event. The resulting map can often represent millions of data points. Traditionally, close intersections between subsets is performed by visual inspection [31]. However, a fast search algorithm for *Poincare* is currently being developed to offer the user the possibility of finding a ranking of intersections automatically. This novel feature is expected to be delivered with the next version.

An illustrative cartoon appears in Fig. 9 showing a surface



(a) Global manifolds in the Earth-Moon system



(b) Zoomed-in view in the vicinity of the Moon

Fig. 8. Stable and unstable manifolds associated with a planar L_1 Lyapunov orbit in the Earth-Moon system.

of section, Σ , and records each time two trajectories cross it. A periodic orbit, Γ , will intersect the surface of section at the same point every revolution, creating ‘fixed points’ in the map. However, manifold trajectory intersections will occur at various parts of the map, depending on the stability of the orbit, and can then be used for a variety of applications. That is, for unstable manifold trajectories, subsequent returns to the map diverge from the original fixed point corresponding to the periodic orbits; conversely, for stable manifold trajectories, recurring crossings of the map approach the original point. If there is no detectable pattern, then the orbit is labeled chaotic.

There are benefits and drawbacks of using Poincaré maps in a visual manner. The main benefit is that, by defining events, the dimensionality of the system is reduced, allowing certain aspects of the system to be more conceptually understandable. Since any particular state is fully defined

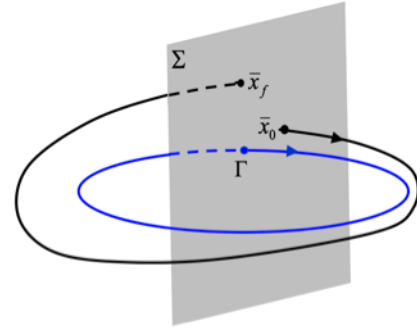


Fig. 9. Schematic representation of a Poincaré map.

with six variables, visualizing six dimensions without missing information is rather difficult, if not virtually impossible. In this case, reducing dimensionality can not only allow for more conceptual clarity, but it can also reveal dynamic structures that were not apparent in the higher-dimension visualizations [25]. The main drawback, however, is that this simplification can yield deceptive visualizations that are not providing any information on the other dimensions.

Specific to *Poincare* and the work that mission designers typically carry out at JPL, the most useful application for these mapping techniques is finding intersections between stable and unstable manifold trajectories. If a connection can be identified, creating a heteroclinic connection [32] between two orbits in a multi-body system via natural dynamic structures can yield low-cost, or in some cases ΔV -free transfers. To date, available types of maps in *Poincare* include user-specified surfaces of section, periapsis, apoapsis, and close-pass (or flybys) maps. However, hooks exist to easily define any other type of map.

Once the manifold trajectories for two selected orbits (e.g., arrival and departure) have been numerically integrated and the corresponding Poincaré maps have been created, the user can then visualize the resulting map and search for potential intersections or areas of interest. Alternatively, the user can let the KD-Tree search algorithm implemented in *Poincare* find the nearest-neighbor within the data structure. As an illustrative example, consider the L_1 and L_2 halo orbits at the same energy level plotted in the upper left corner of Fig. 10. With *Poincare*’s manifold module, 100,000 stable and 100,000 unstable manifold trajectories are propagated backwards/forward in time for 200 days and every intersection with the x -axis is recorded and stored. The stored data sets can then be filtered by a number of user-defined constraints, e.g., maximum position discontinuity between points on the maps < 100 km, maximum time-of-flight < 150 days, and transfer $\Delta V < 5$ m/s. Using the KD-Tree algorithm, the filtered solutions can now be ranked according to the search criteria. The user can either retrieve the top solutions in a standard BOA format or can visually interact with the filtered map to evaluate — and either accept or discard — the

set of lowest- ΔV connections between stable and unstable manifolds (Fig. 10.)

Simply put, KD-Trees are built from the SciPy KD-Tree functionality [34] and are created from the set of all unstable points on a map; a nearest neighbor function is then executed for each point in the other data set (stable points) in order to find the globally closest points between these two distinct sets. Computationally, this reduces the time complexity of the search from the $O(n^2)$ brute force approach, to a more manageable $O(n \log n)$ approach [35]. As mentioned earlier, this novel automatic search feature is currently in the prototype stage, but it is expected to be delivered in the near future.

5. SUMMARY

Mission designers are often faced with the task to explore multiple possible destinations, to or from a science orbit, that fit within time of flight and propellant constraints. A relatively recent technique to do so involves leveraging low energy multi-body dynamical technique to produce low-cost, or even ΔV -free transfers. *Poincare* is a MONTE trajectory design tool that allows users to easily interact with these sorts of three-body science orbits and dynamic structures across various multi-body systems. While much of the theory regarding how to compute and connect such orbits is pre-existing and well-understood, this is something that has not yet been made available in a user-friendly way and within an all-in-one environment in MONTE. The different *Poincare* modules allow mission designers to not only explore potentially desirable science orbits, but also have the ability to find connections within the system, and eventually create complete end-to-end high-fidelity reference trajectories to satisfy a set of science requirements.

6. ACKNOWLEDGMENT

The authors wish to acknowledge and thank Nick Lafarge for his contributions to this project during his 2017 summer internship in the Mission Design and Navigation Section at JPL. This research was carried out at the Jet Propulsion Laboratory, California Institute of Technology, under a contract with the National Aeronautics and Space Administration. © 2018 California Institute of Technology. Government sponsorship acknowledged.

7. REFERENCES

- [1] V. Domingo, B. Fleck, and A. I. Poland, “The SOHO Mission: An Overview,” *Solar Physics*, vol. 162, pp. 1–37, 1995.
- [2] P. Sharer and T. Harrington, “Trajectory Optimization for the ACE Halo Orbit Mission,” in *AAS/AIAA Astrodynamics Specialist Conference*, San Diego, California, 29-31 July 1996, Paper AAS 93-3601.
- [3] C. L. Bennett, M. Bay, M. Halpern, G. Hinshaw, C. Jackson, N. Jarosik, A. Kogut, M. Limon, S. S. Meyer, L. Page, D. N. Spergel, G. S. Tucker, D. T. Wilkinson, E. Wollack, and E. L. Wright, “The Microwave Anisotropy Probe Mission,” *Astrophysical Journal*, vol. 583, pp. 1–23, January 2003.
- [4] C. Conley, “Low Energy Transit Orbits in the Restricted Three-Body Problem,” *SIAM Journal of Applied Mathematics*, vol. 16, pp. 732–746, 1968.
- [5] M. Vaquero and K. C. Howell, “Design of Transfer Trajectories Between Resonant Orbits in the Earth-Moon Restricted Problem,” *Acta Astronautica*, May 2013, Available at: <http://dx.doi.org/10.1016/j.actaastro.2013.05.006>.
- [6] M. Vaquero and K. C. Howell, “Transfer Design Exploiting Resonant Orbits and Manifolds in the Saturn-Titan System,” *Journal of Spacecraft and Rockets*, February 2013, DOI: 10.2514/1.A32412.
- [7] NASA Jet Propulsion Laboratory, “NEO-Cam Finding Asteroids before They Find Us,” <https://neocam.ipac.caltech.edu>, 2017.
- [8] M. Swain, “Finesse - A New Mission Concept For Exoplanet Spectroscopy,” in *AAS/Division for Planetary Sciences Meeting Abstracts #42*, Oct. 2010, vol. 42 of *Bulletin of the American Astronomical Society*, p. 1064.
- [9] T. Gauron C. Heneghan M. Holman A. Kenter R. Kraft J. Livingstone R. Murray-Clay P Nulsen M. Payne H. Schlichting A. Trangsrud J. Vrtilek C. Alcock, M. Brown and M. Werner, “The Whipple Mission: Exploring the Kuiper Belt and the Oort Cloud,” in *AAS/Division for Planetary Sciences Meeting Abstracts #47*, Nov. 2015, vol. 47 of *AAS/Division for Planetary Sciences Meeting Abstracts*, p. 312.07.
- [10] J. Parker, T. McElrath, R. Anderson, and T. Sweetser, “Trajectory Design for Moonrise: a Proposed Lunar South Pole-Aitken Basin Sample Return Mission,” in *AAS/AIAA Astrodynamics Specialist Conference*, Hilton Head, South Carolina, 11-15 August 2013, Paper AAS-13-4849.
- [11] M. McGuire, N. Strange, L. Burke, L. McCarty, G. Lantoine, M. Qu, H. Shen, D. Smith, and M. Vavrina, “Overview of the Mission Design Reference Trajectory for NASA’s Asteroid Redirect Robotic Mission,” in *AAS/AIAA Astrodynamics Specialist Conference*, Stevenson, Washington, 20-24 August 2017, Paper AAS-17-585.

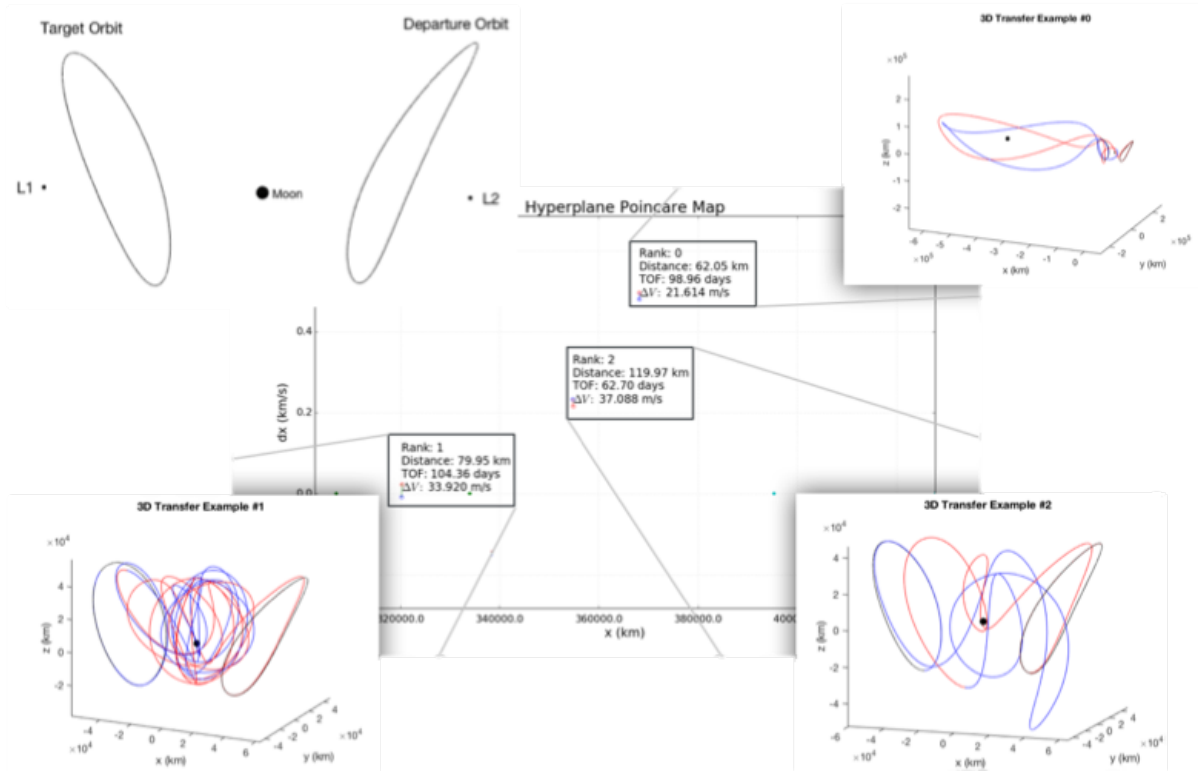


Fig. 10. Same energy level, three-dimensional halo orbits in the Earth-Moon system (top left); filtered Poincaré map representing the intersections of the stable and unstable manifolds associated with the selected L_1 and L_2 halo orbits ranked by ΔV (center); various geometries for initial guesses found by KD-Tree algorithm (top right, bottom right, bottom left plots) [33].

- [12] M. Vaquero and J. Senent, “An Efficient Method to Design Premature End-Of-Life Trajectories: A Hypothetical Alternate Fate for Cassini,” in *25th International Symposium on Space Flight Dynamics*, Munich, Germany, 19-23 October 2015.
- [13] Mission Design and Navigation Section, NASA Jet Propulsion Laboratory, “Mission Analysis Operations and Navigation Toolkit Environment,” vol. JPL 400-1640, July, 2016.
- [14] J. Smith, W. Taber, T. Drain, S. Evans, J. Evans, M. Guevara, W. Schulze, R. Sunseri, and H. Wu, “MONTE Python for Deep Space Navigation,” in *Proceedings of the 15th Python in Science Conference (SciPy 2016)*, Austin, Texas, 11-17 July 2016.
- [15] S. Evans, “MONTE: The Next Generation of Mission Design and Navigation Software,” in *The 6th International Conference on Astrodynamics Tools and Techniques (ICATT) proceedings 2016*, Darmstadt, Germany, 2016.
- [16] V. Szebehely, *Theory of Orbits: The Restricted Problem of Three Bodies*, 1967.
- [17] H. Poincaré, *Les Méthodes Nouvelles de la Mécanique Celeste*, vol. II, Gauthier-Villars, Paris, 1892.
- [18] R. Broucke, “Stability of Periodic Orbits in the Elliptic, Restricted Three-Body Problem,” *American Institute of Aeronautics and Astronautics Journal*, vol. 7, no. 6, pp. 1003, June 1969.
- [19] E. J. Doedel et al., “Elemental Periodic Orbits Associated with the Libration Points in the Circular Restricted 3-Body Problem,” *International Journal of Bifurcation and Chaos*, vol. 17, no. 8, pp. 2625–2677, January 2007.
- [20] D. J. Grebow, “Generating Periodic Orbits in the Circular Restricted Three-Body Problem with Applications to Lunar South Pole Coverage,” M.S. Thesis, School of Aeronautics and Astronautics, Purdue University, West Lafayette, Indiana, 2006.
- [21] D. Guzzetti, N. Bosanac, A. Haapala, K. Howell, and D. Folta, “Rapid Trajectory Design in the Earth-Moon Ephemeris System via an Interactive Catalog of Periodic and Quasi-Periodic Orbits,” *Acta Astronautica*, pp. 439–455, September-October 2016.
- [22] A. Leiva and C. Briozzo, “The Earth-Moon CR3BP:

- A Full Atlas of Low-Energy Fast Periodic Transfer Orbits,” *Celestial Mechanics and Dynamical Astronomy*, December 2006.
- [23] D. Folta, N. Bosanac, D. Guzzetti, and K. Howell, “An Earth-Moon System Trajectory Design Reference Catalog,” in *2nd IAA Conference on Dynamics and Control of Space Systems (DYCOSS)*, Roma, Italy, 24-26 March 2014, Paper ID 37.
- [24] R. Restrepo and R. Russell, “A Database of Planar Axisymmetric Periodic Orbits for the Solar System,” *Celestial Mechanics and Dynamical Astronomy*, vol. 130, pp. 49, July 2018.
- [25] M. Vaquero, “Spacecraft Transfer Trajectory Design Exploiting Resonant Orbits in Multi-Body Environments,” Ph.D. Dissertation, School of Aeronautics and Astronautics, Purdue University, West Lafayette, Indiana, 2013.
- [26] V. A. Yakubovich and V. M. Starzhinskii, *Differential Equations with Periodic Coefficients*, John Wiley and Sons, New York, 1975.
- [27] K. C. Howell, “Three-dimensional, Periodic, ‘Halo’ Orbits,” *Celestial Mechanics*, vol. 32, no. 1, pp. 53–71, January 1984.
- [28] D. J. Grebow, “Trajectory Design in the Earth-Moon System and Lunar South Pole Coverage,” Ph.D. Dissertation, School of Aeronautics and Astronautics, Purdue University, West Lafayette, Indiana, 2010.
- [29] Mission Design and Navigation, NASA Jet Propulsion Laboratory, “Mission Analysis, Operations, and Navigation Toolkit Environment,” <https://montepy.jpl.nasa.gov/>.
- [30] M. Vaquero and K. Howell, “Poincaré Maps and Resonant Orbits in the Circular Restricted Three-Body Problem,” in *AAS/AIAA Astrodynamics Specialist Conference*, Girdwood, Alaska, July-August 2011, Paper AAS-11-428.
- [31] K. Howell, D. Davis, and A. Haapala, “Application of Periapse Maps for the Design of Trajectories Near the Smaller Primary in Multi-Body Regimes,” .
- [32] M. Vaquero, “Poincaré Sections and Resonant Orbits in the Restricted Three-Body Problem,” M.S. Thesis, School of Aeronautics and Astronautics, Purdue University, West Lafayette, Indiana, 2010.
- [33] N. Lafarge, “A Monte.Poincare Interactive Tool for Computing Orbit Connections,” in *Final Report, Jet Propulsion Laboratory Summer Internship Program*, August 2017.
- [34] SciPy.org, “SciPy KDTree Documentation,” <https://docs.scipy.org/doc/scipy-0.14.0/reference/generated/scipy.spatial.KDTree.html>, 2014.
- [35] S. Maneewongvatana and D. M. Mount, “On the Efficiency of Nearest Neighbor Searching with Data Clustered in Lower Dimensions,” in *International Conference on Computational Science (ICCS’01)*, 2001.